



# Journal of Applied Sciences

ISSN 1812-5654

**science**  
alert

**ANSI***net*  
an open access publisher  
<http://ansinet.com>

## An Inverse Solution for 2D Electrical Impedance Tomography Based on Electrical Properties of Material Blocks

A. Abbasi, B. Vosoughi Vahdat and Gh. Ebrahimi Fakhim  
 Department of Electrical Engineering,  
 Sharif University of Technology, Tehran, Iran

**Abstract:** The present study provides an inverse solution and analysis on a new approach for Electrical Impedance Tomography (EIT) process as block method in EIT. In this method, it is assumed that all of the particles of each block have the same electrical properties (electrical conductivities). This technique is used to enhance image resolution and also to improve reconstruction algorithm. Although this method has been developed for 3D objects, in this study it is assumed that the subject has a (two-dimensional) rectangular shape and is made of fixed size blocks. By considering the previous conditions and computing relationship among currents, voltages and electrical impedances of blocks, the required equations to solve the problem is generated. Computer simulations show that employing the block method in reconstruction algorithm results in more accurate identification.

**Key words:** Electrical impedance tomography, inverse problem, electrical conductivity, medical imaging

### INTRODUCTION

There are a variety of medical applications for which it would be useful to know the distribution of electrical properties inside the body. Electrical conductivity and permittivity are electrical properties and both of these properties are of interest in the medical applications (Cheney *et al.*, 1999). Different tissues have different conductivities and permittivities, on the other hand, the knowledge of the map of the internal electrical properties has a number of advantages in the many of medical diagnosis. EIT is a useful method for medical imaging of pulmonary emboli and blood clots in the lungs, (Cheney *et al.*, 1999; Frerichs, 2000; Frerichs *et al.*, 2002) breast (Osterman *et al.*, 2000; Hartov *et al.*, 2004; Ijaz *et al.*, 2007), neural system studies (Tower, 2000; Polydorides *et al.*, 2002), breath system studies (Li *et al.*, 1996; Metherall, 1998; Putensen *et al.*, 2007; Wu *et al.*, 2007; Lionheart *et al.*, 2008), vascular system studies (Halter *et al.*, 2008), brain imaging (Ansheng *et al.*, 2008) and other medical issues.

It has been shown that the block method approach, improves the results in EIT (Vosoughi and Niknam, 2003). In this study, the EIT problem in 2D format with block method has been defined and after driving necessary equations, a complete non-iterative solution for the problem has been presented. Mathematical proofs and the simulation results have validated the algorithm.

### DEFINITION OF THE MODEL

To generate an EIT image, a series of electrodes are attached to a subject. Various currents can be injected through these electrodes and the produced voltages can be measured. By currents injecting, measuring voltages and using reconstruction algorithm, the conductivity distribution inside the subject would be determined (Lionheart, 2004; Holder, 2004; Babaeizadeh *et al.*, 2007). EIT forward problem involves constructing a block model and calculating the voltages (or currents) produced on the boundary when currents are injected (or voltages are applied) on the same boundary (Babaeizadeh *et al.*, 2007).

Figure 1 shows the description of EIT problem by block method, in which the subject has a rectangular shape divided into  $m \times n$  similar size blocks.

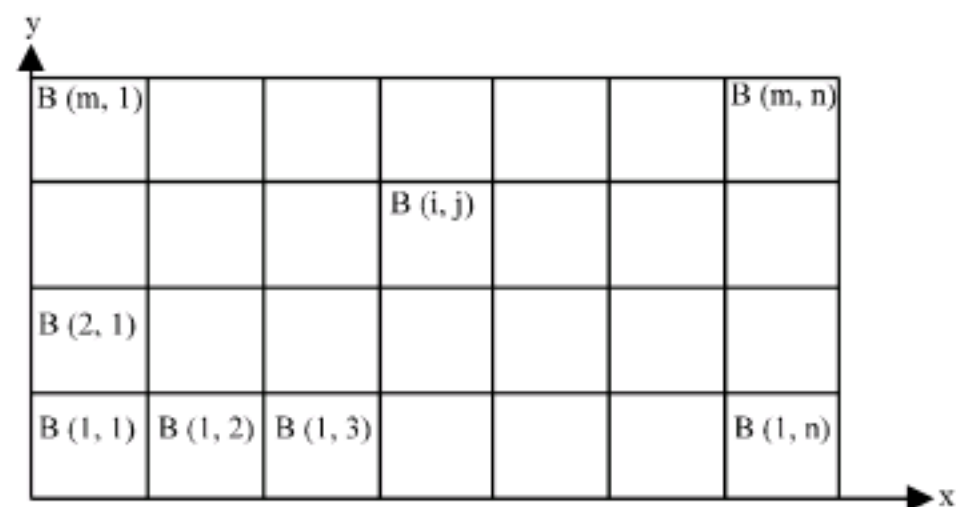


Fig. 1: A schematic of a rectangular shape subject divided to  $m \times n$  similar blocks



It is assumed that all of the particles of a block have the same electrical impedances and also the variation of the current densities within a block is linear (Vosoughi and Niknam, 2003). This assumption can be true, when  $m, n \rightarrow \infty$ .

In Fig. 1, the rectangular subject has been aligned in Cartesian system, so, it is possible to assign a number for each block as  $B(i, j)$  (block in  $i$ th row and  $j$ th column). For a single block,  $J_x(i, j), J_x(i, j+1), J_y(i, j)$  and  $J_y(i+1, j)$  are current density components and  $e_x(i, j), e_x(i, j+1), e_y(i, j)$  and  $e_y(i+1, j)$  are voltage components for  $B(i, j)$  and  $\sigma(i, j)$  is specific conductivity in hole parts of  $B(i, j)$  (Fig. 2a) where,  $J_x(i, j)$  and  $J_y(i, j)$  are the current densities entering the  $B(i, j)$  block from X and Y directions, respectively. Similarly,  $e_x(i, j)$  and  $e_y(i, j)$  are the voltages of the edge-centers for the  $B(i, j)$  block.  $\Delta_x$  and  $\Delta_y$  are the lengths of a block in X and Y directions, respectively (Fig. 2b). Since choosing the block size is arbitrary, set  $\Delta_x = \Delta_y = \Delta$ .

Inside the block, the current density can be written as:

$$J_x(i, j) = J_x(i, j+1) + \frac{\hat{x} - \Delta}{\Delta} [J_x(i, j+1) - J_x(i, j)] \quad (1)$$

$$J_y(i, j) = J_y(i+1, j) + \frac{\hat{y} - \Delta}{\Delta} [J_y(i+1, j) - J_y(i, j)] \quad (2)$$

where,  $\hat{x}$  and  $\hat{y}$  are distances from the primary edges of the block  $B(i, j)$  in X and Y directions, respectively. According to the Ohm's law  $\vec{j} = \sigma \vec{E} = -\sigma \nabla V$  the potential values of the block  $B(i, j)$  can be obtained as the followings:

$$e_x(i, j) - e_x(i, j+1) = - \int_0^{\hat{x}} \frac{1}{\sigma(i, j)} J_x(i, j) d\hat{x} \quad (3)$$

$$= - \frac{1}{2} \left( \frac{J_x(i, j+1) - J_x(i, j)}{\sigma(i, j)\Delta} \right) \hat{x}^2 - \frac{J_x(i, j)}{\sigma(i, j)} \hat{x}$$

$$e_y(i, j) - e_y(i, j+1) = - \int_0^{\hat{y}} \frac{1}{\sigma(i, j)} J_y(i, j) d\hat{y} \quad (4)$$

$$= - \frac{1}{2} \left( \frac{J_y(i+1, j) - J_y(i, j)}{\sigma(i, j)\Delta} \right) \hat{y}^2 - \frac{J_y(i, j)}{\sigma(i, j)} \hat{y}$$

Particularly the following equations can be obtained:

$$e_x(i, j) - e_x(i, j+1) = \frac{1}{2} \Delta \frac{J_x(i, j) + J_x(i, j+1)}{\sigma(i, j)} \quad (5)$$

$$e_y(i, j) - e_y(i+1, j) = \frac{1}{2} \Delta \frac{J_y(i, j) + J_y(i+1, j)}{\sigma(i, j)} \quad (6)$$

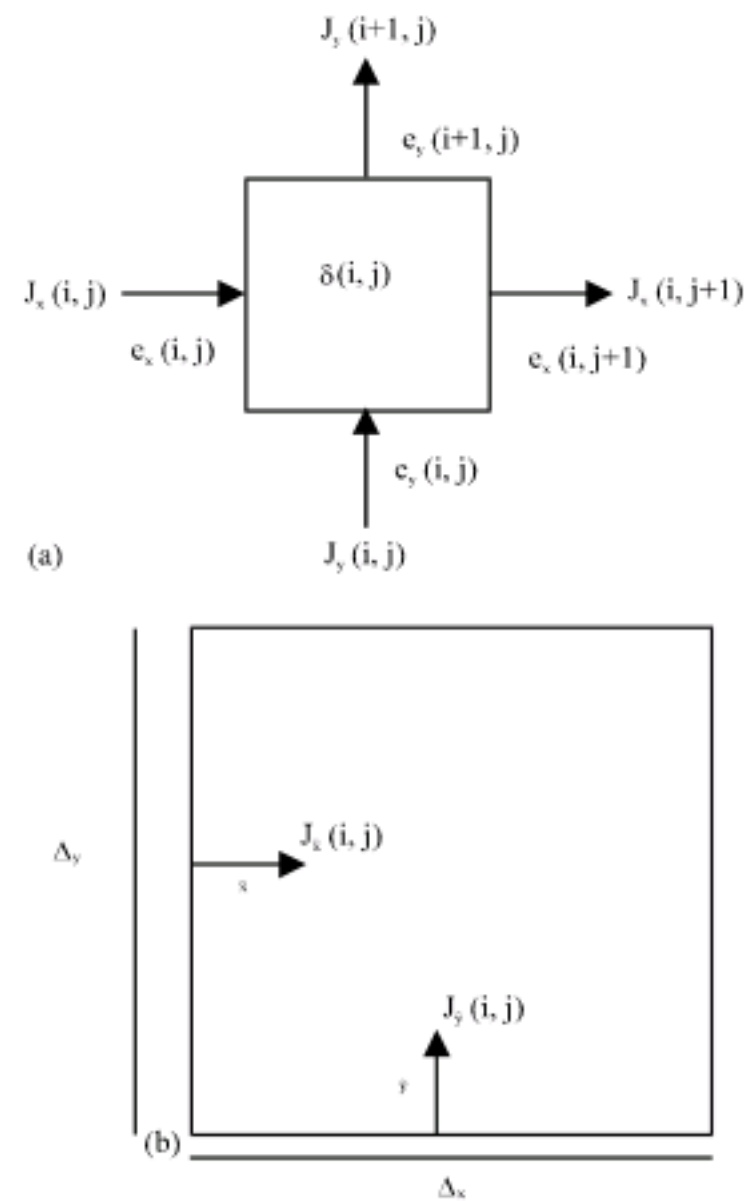


Fig. 2: (a) Block  $B(i, j)$  with  $\sigma(i, j)$  specific conductivity and its current and voltage components and (b) current distribution in block  $B(i, j)$  and sides' size of block

In forward problem of EIT,  $\sigma(i, j)$  are known. If the current densities on the boundaries are known the voltages on the same boundaries could be found. On the other hand if the voltages on the boundaries are known the current densities on the same boundaries could be found. To solve the forward problem in block method the following equations are used:

$$e_x(i, j+1) = e_x(i, j) - \frac{1}{2} \Delta \frac{J_x(i, j) + J_x(i, j+1)}{\sigma(i, j)} \quad (7)$$

$$e_y(i+1, j) = e_y(i, j) - \frac{1}{2} \Delta \frac{J_y(i, j) + J_y(i+1, j)}{\sigma(i, j)} \quad (8)$$

$$\text{KCL: } J_x(i, j) + J_y(i, j) = J_x(i, j+1) + J_y(i+1, j) \quad (9)$$

$$\text{KVL: } e_x(i, j) - e_y(i, j) = \frac{1}{8} \frac{\Delta}{\sigma(i, j)} (3J_x(i, j) + J_x(i, j+1) - 3J_y(i, j) - J_y(i+1, j)) \quad (10)$$

$$i \in N, 1 \leq i \leq m \text{ and } j \in N, 1 \leq j \leq n$$



Kirchhoff's Current Law (KCL) and Kirchhoff's Voltage Law (KVL) are two fundamental laws in electrical engineering. KCL implies that: at any point in an electrical circuit that does not represent a capacitor plate; the sum of currents flowing towards that point is equal to the sum of currents flowing away from that point. KVL implies that: the directed sum of the electrical potential differences around any closed circuit must be zero. Equation 10 has been developed by addition of  $e_x(i, j) - e_0(i, j)$  and  $e_0(i, j) - e_y(i, j)$  where,  $e_0(i, j)$  is voltage of B(i, j) in centre of the block. In forward problem of EIT  $e_x(i, j+1)$ ,  $e_y(i, j+1)$ ,  $J_x(i, j+1)$  and  $J_y(i, j+1)$  can be calculated from four independent equations (Eq. 7-10).

**PROPOSED INVERSE SOLUTION**

The block method employed in this study, is a new approach. Forward problem solution by block method has been discussed previously (Vosoughi and Niknam, 2003; Vahdat, 2004; Abbasi *et al.*, 2007). In this study an inverse solution is introduced for the block method. In inverse problem of EIT, currents and voltages of boundaries are known and  $\sigma(i, j)$  of blocks would be calculated. For a subject with  $m \times n$  blocks (Fig. 1), in the first row from B(1, 1) to B(1, n) the following equations can be obtained:

$$\sigma(1, j)e_x(1, j) - 2\sigma(1, j)e_y(1, j) + \sigma(1, j)e_x(1, j+1) + \Delta J_y(1, j) = 0 \quad (11)$$

where,  $e_x(1, 1)$ ,  $J_x(1, 1)$ ,  $e_x(1, n+1)$ ,  $J_x(1, n+1)$ ,  $e_y(1, j)$  and  $\Delta J_y(1, j)$  are known.  $\sigma(1, j)$  and  $e_x(1, j)$  are the unknown parameters.

Equation 11 generates n equations with  $n+(n-1) = 2n-1$  unknown parameters for the first row where unknown parameters are  $\sigma(1, j)$  and  $e_x(1, j)$ . If the test is repeated in the first row by new currents and voltages of boundaries, new n equations with  $2n-1$  unknown parameters would be obtained. It should be known that  $\sigma(1, j)$  are the same in all tests, while  $e_x(1, j)$  are different in each test. Counting the number of parameters, it would be clear that a new test adds only n-1 new unknown parameters. Therefore, every test adds n equations and n-1 new unknown parameters. If the test is repeated for n times,  $n^2$  equations and  $n+n(n-1) = n^2$  unknown parameters are obtained.  $n^2$  unknown parameters can be solved by numerical methods and n for  $n^2$  of the first row can be found.

For the second row from B(2, 1) to B(2, n), the boundary values of this row from the n previously achieved tests is needed. Boundary values  $e_x(2, 1)$ ,  $J_x(2, 1)$ ,  $e_x(2, n+1)$  and  $J_x(2, n+1)$  are known from the measurements.  $e_y(2, j)$  and  $J_y(2, j)$  are calculated by following equations for n test.

$$\Delta J_y(2, j) = 2\Delta J_x(1, j) - \Delta J_y(1, j) - 4\sigma(1, j)e_x(1, j) + 4\sigma(1, j)e_y(1, j) \quad (12)$$

$$e_y(2, j) = e_y(1, j) - \frac{1}{2} \Delta \frac{J_y(1, j) + J_y(2, j)}{\sigma(1, j)} \quad (13)$$

Now,  $\sigma(2, j)$  from  $n^2$  equations in the second row can be calculated. To find the parameters of all blocks, this procedure can be repeated for all rows. With n tests,  $n^2$  equations are available in each row and by solving these equations the conductivities would be obtained.

MATLAB version 7.0.0 is used for simulating the method. The algorithm consists of two parts. In the first part, using the EIT forward solution a phantom model is constructed with known boundary values. In the second part, using the data in the first part inverse problem is solved. In the first part the following steps will be obtained:

- Getting row-number and column-number
- Generating  $\sigma(i, j)$  randomly between 0 and 255 for all blocks
- Generating  $J_x(i, 1)$ ,  $J_y(i, j)$ ,  $e_x(i, 1)$  and  $e_y(i, j)$  randomly
- Calculating  $J_x(i, j)$ ,  $J_y(i, j)$ ,  $e_x(i, j)$  and  $e_y(i, j)$  by the steps 2 and 3, using Eq. 7-10
- Repeating steps 3 and 4 to generate enough tests

The next part of the algorithm is the inverse solution. In this part using the boundary values of currents and voltages,  $\sigma(i, j)$  are calculated. The solve function of MATLAB is used for nonlinear equation solution (equation 11) through the following steps:

- Using the boundary values and solve function for the first row ( $\sigma(1, j)$  in the first row would result)
- Using Eq. 12 and 13 and calculating boundary conditions for the second row
- Using steps 1 for the second row and calculating  $\sigma(2, j)$
- Repeating steps 2 and 3 for all of the other rows

**SIMULATION**

Here, two examples for a  $5 \times 5$  block (25 unknown  $\sigma(i, j)$ ) and a  $4 \times 7$  block (28 unknown  $\sigma(i, j)$ ) is presented. Dimensions of examples are suitable for proving inverse algorithm accuracy. Fast and powerful computers should be used for greater dimensions.

Figure 3 shows the result of applying this algorithm for a  $5 \times 5$  block. Figure 3a is the distribution of real  $\sigma(i, j)$  which is generated by forward algorithm.  $\sigma(i, j)$  for blocks



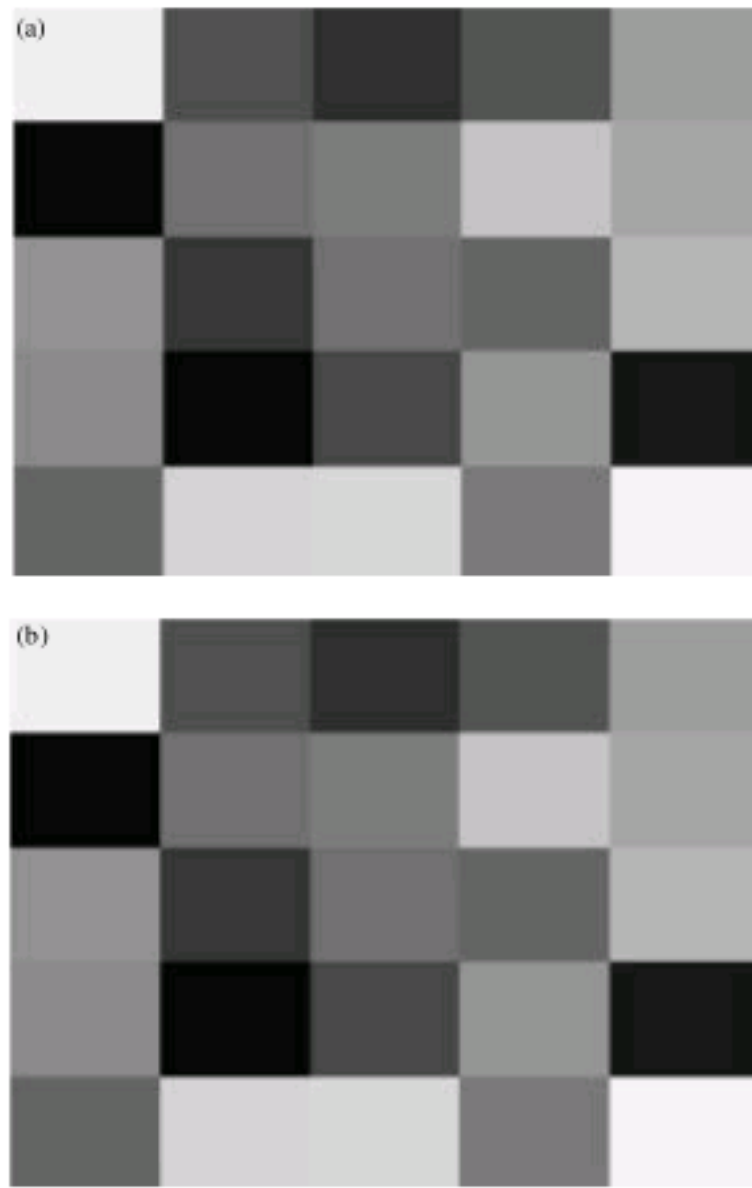


Fig. 3: (a) distribution of real  $\sigma(i, j)$  for  $5 \times 5$  block and (b) distribution of calculated  $\sigma(i, j)$  for  $5 \times 5$  block

are randomly selected.  $\sigma(i, j)$  are random floating point values between 0-255 where white and black colours describe 0 and 255, respectively. Figure 3b is the result of inverse algorithm and shows distribution of calculated  $\sigma(i, j)$ . Inverse algorithm has used the generated boundary conditions of forward algorithm. On the other hand for Fig. 3a and b boundary conditions are the same. In this example there are 25 blocks and inverse algorithm calculates 25  $\sigma(i, j)$ .

Root Mean Square Error (RMSE) has been used to compare real and calculated values of a variable. For this example according to the following formula, RMSE equals to  $1.116 \times 10^{-4}$ . The small value of the error compared to real conductivity distributions shows the accuracy of the algorithm.

$$RMSE = \sqrt{\frac{\sum_{i=1}^m \sum_{j=1}^n (\sigma_r(i, j) - \sigma_c(i, j))^2}{m \times n}} \quad (14)$$

where,  $\sigma_r(i, j)$  and  $\sigma_c(i, j)$  are the real and calculated conductivities respectively. Also for this example maximum difference between the values of  $\sigma_r(i, j)$  and  $\sigma_c(i, j)$  is  $4.421 \times 10^{-4}$ .

Next example is for a  $4 \times 7$  block. Figure 4a and b show distribution of the real and calculated  $\sigma(i, j)$ . In forward algorithm  $\sigma(i, j)$  for blocks has been selected random



Fig. 4: (a) distribution of real  $\sigma(i, j)$  for  $4 \times 7$  block and (b) distribution of calculated  $\sigma(i, j)$  for  $4 \times 7$  block

floating point values between 0 to 255. For Fig. 4a and b boundary conditions are the same and there are 28 blocks, so inverse algorithm is calculating 28  $\sigma(i, j)$ . Root mean square error for this example equals to  $6.193 \times 10^{-5}$ . Order of RMSE for similar examples with different random  $\sigma(i, j)$  is about  $10^{-5}$  to  $10^{-4}$  which shows accuracy of inverse reconstruction algorithm.

In most algorithms for EIT inverse problem presented in literature, there isn't any numerical or quantitative comparison between real and calculated conductivities. However in some papers RMSE has been a comparison factor. For example in a work conducted by Kim *et al.* (2006a) for 2D EIT inverse problem, applying interpolation of front points method for approximation of regions of inner object results in RMSE on order of  $10^{-5}$  to  $10^{-3}$  for reconstructed image. Also, using neural networks and front point approach for estimation of 2D EIT image results  $10^{-2}$  to  $10^{-1}$  in RMSE (Kim *et al.*, 2006b). Tossavainen and *et. al* applied shape estimation and state estimation formulation for a dynamic EIT problem and reported RMSE from  $10^{-1}$  to 10 in conductivity (Tossavainen *et al.*, 2006). In other work conducted by Ijaz, a dynamic reconstruction algorithm has been presented to monitor the concentration distribution Inside the fluid vessel based on EIT by employing interacting Multiple Model (IMM), Extended Kalman Filtering (EKF) and covariance Compensation Extended Kalman Filtering



Table 1: RMSE comparison between methods

Algorithm for EIT	RMSE
Shape estimation and state estimation for dynamic EIT (Tossavainen <i>et al.</i> , 2006)	$10^{-1}$ -10
Shape estimation by EKF for dynamic EIT (Ijaz and Kim, 2006)	$10^{-2}$ - $10^{-1}$
Employing IMM, EKF and CCEKF for dynamic EIT (Ijaz <i>et al.</i> , 2006)	$10^{-2}$ - $10^{-1}$
Neural networks and front point approach (Kim <i>et al.</i> , 2006b)	$10^{-2}$ - $10^{-1}$
Interpolation of front points method (Kim <i>et al.</i> , 2006a)	$10^{-5}$ - $10^{-3}$
Block method (present study)	$10^{-5}$ - $10^{-4}$

(CCEKF). For this study RMSE of conductivity has been reported between  $10^{-2}$  to  $10^{-1}$  (Ijaz *et al.*, 2006). Using shape estimation of regions of known resistivities based on extended Kalman filtering for dynamic EIT results in RMSE from  $10^{-2}$  to  $10^{-1}$  (Ijaz and Kim, 2006). Table 1 represents these results:

Therefore RMSE from  $10^{-5}$  to  $10^{-4}$  for this method is in a proper order and indicates that real and calculated conductivities are almost the same.

### CONCLUSION AND RECOMMENDATIONS

The proposed method is an accurate solution for 2D electrical impedance tomography. Low error and high resolution of this method is clear. This method can lead a great step in EIT problem solution. Although this method is theoretical, it may have better results than other common ways in literature.

Linear solution for EIT inverse problem and also development of this method from 2D to 3D can be suggested as new field for future investigations.

### REFERENCES

Abbasi, A., F. Pashakhanlou and B.V. Vahdat, 2007. Error propagation in non-iterative eit block method. Proceedings of the IEEE International Symposium on Signal Processing and Information Technology, Dec. 15-18, IEEE Xplore London, pp: 678-681.

Ansheng, N., T. Chi, Y. Guosheng, F. Feng and D. Xiuzhen, 2008. Effect of skull inhomogeneities on localization accuracy in brain electrical impedance tomography. Proceedings of IEEE 2nd International Conference on Bioinformatics and Biomedical Engineering, May 16-18, Shanghai, pp: 2705-2707.

Babaeizadeh, S., D.H. Brooks and D. Isaacson, 2007. 3-D Electrical impedance tomography for piecewise constant domains with known internal boundaries. IEEE Trans. Biomed. Eng., 54: 2-10.

Cheney, M., D. Isaacson and J.C. Newell, 1999. Electrical impedance tomography. Siam Rev., 41: 85-101.

Frerichs, I., 2000. Electrical impedance tomography (EIT) in applications related to lung and ventilation: A review of experimental and clinical activities. Physiol. Meas., 21: 1-21.

Frerichs, I., J. Hinz, P. Herrmann, G. Weisser, G. Hahn, M. Quintel and G. Hellige, 2002. Regional lung perfusion as determined by electrical impedance tomography in comparison with electron beam ct imaging. IEEE Trans. Med. Imagin Public, 21: 646-652.

Halter, R., A. Hartov and K. Paulsen, 2008. Video rate electrical impedance tomography of vascular changes: Preclinical development. Physiol. Meas., 29: 349-364.

Hartov, A., N.K. Soni and K.D. Paulsen, 2004. Variation in breast Eit measurements due to menstrual cycle. Physiol. Meas., 25: 295-299.

Holder, D.S., 2004. Electrical Impedance Tomography: Methods, History and Applications. Series in Medical Physics and Biomedical Engineering. 1st Edn., Institute of Physics, Bristol., ISBN: 0750309520, pp: 63-64.

Ijaz, U.Z. and K.Y. Kim, 2006. Kinematic models for non-stationary elliptic region boundary in electrical impedance tomography. J. Res. Instit. Adv. Technol., 17: 25-32.

Ijaz, U.Z., J.H. Kim, A.K. Khambampati, M.C. Kim, S. Kim and K.Y. Kim, 2007. Concentration distribution estimation of fluid through electrical impedance tomography based on interacting multiple model scheme. Flow Measure. Instrument., 18: 47-56.

Ijaz, U.Z., S.K. Bong, K. Tzu-Jen, A.K. Khambampati and S. Kim *et al.*, 2008. Mammography phantom studies using 3D electrical impedance tomography with numerical forward solver. Proceedings of the IEEE, Frontiers in the Convergence of Bioscience and Information Technologies, Oct. 11-13, Jeju City, pp: 379-383.

Kim, J.H., B.C. Kang, S.H. Lee, B.I. Choi and M.C. Kim *et al.*, 2006. Phase boundary estimation in electrical resistance tomography with weighted multi-layered neural networks and front point approach. Meas. Sci. Technol., 17: 2731-2739.

Kim, M.C., S. Kim, K.Y. Kim, K.H. Seo, H.J. Jeon, J.H. Kim and B.Y. Choi, 2006. Estimation of phase boundary by front points method in electrical impedance tomography. Inverse Prob. Sci. Eng., 14: 455-466.

Li, J.H., C. Joppek and U. Faust, 1996. Fast eit data acquisition system with active electrodes and its application to cardiac imaging. Physiol. Meas., 17: 25-32.



- Lionheart, W.R., 2004. EIT reconstruction algorithms: Pitfalls, challenges and recent developments. *Physiol. Meas.*, 25: 125-142.
- Lionheart, W.R., F.J. Lidgey, C.N. Mcleod, K.S. Paulson, M.K. Pidcock and Y. Shi, 2008. Electrical impedance tomography for high speed chest imaging. *Physica. Med.*, 13: 247-249.
- Metherall, P., 1998. Three dimensional electrical impedance tomography of the human thorax. Ph.D Thesis, University of Sheffield.
- Osterman, K.S., T.E. Kerner and D.B. Williams, 2000. Multifrequency electrical impedance imaging: Preliminary *in vivo* experience in breast. *Physiol. Meas.*, 21: 99-110.
- Polydorides, N., W.R. Lionheart and H. McCann, 2002. Krylov subspace iterative techniques: On the detection of brain activity with electrical impedance tomography. *IEEE Trans. Med. Imag.*, 21: 596-603.
- Putensen, C., J. Zinserling and H. Wrigge, 2007. *Electrical Impedance Tomography for Monitoring of Regional Ventilation in Critically Ill Patients*. 1st Edn., Springer Berlin Heidelberg, New York.
- Tossavainen, O.P., M. Vauhkonen, V. Kolehmainen and K.Y. Kim, 2006. Tracking of moving interfaces in sedimentation processes using electrical impedance tomography. *Chem. Eng. J.*, 61: 7717-7729.
- Tower, C.M., 2000. 3D Simulation of EIT for monitoring impedance variations within the human head. *Physiol. Meas.*, 21: 119-124.
- Vahdat, B.V., 2004. Noniterative method to solve 3D EIT forward problem. Proceedings of the 4th IEEE International Symposium on Signal Processing and Information Technology, Dec. 18-21, IEEE Computer Society, London, pp: 449-452.
- Vosoughi, V.B. and G. Niknam, 2003. Block method approach in electrical impedance tomography. Proceedings of the 3rd IEEE International Symposium on Signal Processing and Information Technology, Dec. 14-17, IEEE Computer Society London, pp: 475-478.
- Wu, X., Y. Sun and J. Cen, 2007. Circuit for measuring breath waveform with impedance method and method and device for resisting interference of electrical fast transient. Shenzhen Mindray Bio-Medical Electronics Co. Ltd., USA.